ACCOUNTS
of chemical research

Reactive Ballistic Deposition of Nanostructured Model Materials for Electrochemical Energy Conversion and Storage

DAVID W. FLAHERTY,[†] NATHAN T. HAHN,[†] R. ALAN MAY,[†,‡] SEAN P. BERGLUND,[†] YONG-MAO LIN,[†] KEITH J. STEVENSON,[†] ZDENEK DOHNALEK,[‡] BRUCE D. KAY,[‡] AND C. BUDDIE MULLINS*[,†]

[†]*Departments of Chemical Engineering and Chemistry, Center for Nano- and Molecular Science and Technology, Center for Electrochemistry, and Texas Materials Institute, University of Texas at Austin, 1 University CO400, Austin, Texas 78712-0231, United States, and* [‡]*Pacific Northwest National Laboratory, Fundamental Sciences Directorate, Chemical and Material Sciences Division, P.O. Box 999, K8-88, Richland, Washington, 99352*

RECEIVED ON JUNE 15, 2011

CONSPECTUS

Porous, high surface area materials have critical roles in applications including catalysis, photochemistry, and energy storage. In these fields, researchers have demonstrated that the nanometer-scale structure modifies mechanical, optical, and electrical properties of the material, greatly influencing its behavior and performance.

Such complex chemical systems can involve several distinct processes occurring in series or parallel. Understanding the influence of size and structure on the properties of these materials requires techniques for producing clean, simple model systems. In the fields of photoelectrochemistry and lithium storage, for example, researchers need to evaluate the effects of changing the electrode structure of a single material or producing electrodes of many different candidate materials while maintaining a distinctly favorable morphology.

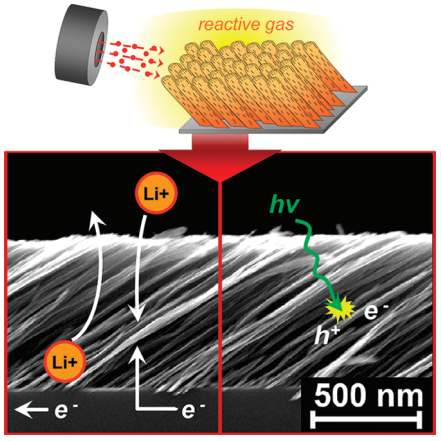

In this Account, we introduce our studies of the formation and characterization of high surface area, porous thin films synthesized by a process called reactive ballistic deposition (RBD). RBD is a simple method that provides control of the morphology, porosity, and surface area of thin films by manipulating the angle at which a metal–vapor flux impinges on the substrate during deposition. This approach is largely independent of the identity of the deposited material and relies upon limited surface diffusion during synthesis, which enables the formation of kinetically trapped structures.

Here, we review our results for the deposition of films from a number of semiconductive materials that are important for applications such as photoelectrochemical water oxidation and lithium ion storage. The use of RBD has enabled us to systematically control individual aspects of both the structure and composition of thin film electrodes in order to probe the effects of each on the performance of the material. We have evaluated the performance of several materials for potential use in these applications and have identified processes that limit their performance. Use of model systems, such as these, for fundamental studies or materials screening processes likely will prove useful in developing new high-performance electrodes.

Finely structured, supported thin films offer a host of opportunities for fundamental and applied research. Nanostructured materials often exhibit physical properties that differ from their bulk counterparts due to the increased importance of the surface in determining the thermodynamics and behavior of the system. Thus, control of the

Published on the Web 10/21/2011 www.pubs.acs.org/accounts
10.1021/ar200164u

characteristic size, porosity, morphology, and surface area presents opportunities to tailor new materials that are useful platforms for elucidating the fundamental processes related to energy conversion and storage.[1,2] The ability to produce high-purity materials with direct control of relevant film parameters such as porosity, film thickness, and film morphology is of immediate interest in the fields of electrochemistry, photocatalysis, and thermal catalysis.[3,4] Studies of various photoactive materials have introduced questions concerning the effects of film architecture and surface structure on the performance of the materials,[5] while recent work has demonstrated that nanostructured, mesoporous, or disordered materials often deform plastically,[6] making them robust in applications where volumetric expansion and phase transformations occur, such as in materials for lithium-ion batteries.[7,8] Moreover, renewed emphasis has been placed on the formation of semiconductive electrodes with controlled pore size and large surface areas for the study and application of pseudocapacitance and cation insertion processes for electrical energy storage.[4] Understanding how the performance of such materials depends on morphology, porosity, and surface structure and area requires a synthesis technique that provides for incremental variations in structure and facilitates assessment of the performance with the appropriate analytical tools, preferably those that provide both structural information and kinetic insight into photoelectrochemical processes.

Here, we describe the application of a method derived from physical vapor deposition (PVD) for the synthesis of thin films that has enabled our studies correlating adsorbent, optical, photochemical, and electrochemical properties of materials with tailored structural characteristics such as morphology, porosity and surface area. We refer to this technique as reactive ballistic deposition (RBD).[9] First, we discuss fundamentals of the growth process, why changes in a single deposition parameter, the deposition angle, result in dramatic changes in film morphology and simple methods for tuning the film composition. Second, we demonstrate how specific aspects of the film structure can be tuned within the RBD deposition scheme. Third, we discuss studies in which RBD grown films were used to deconvolute multiple physical processes, which determine the photochemical behavior, the optical properties of materials, and kinetics of charge storage in electrodes.

The Reactive Ballistic Deposition Process

Thin films are fabricated using a variant of PVD, and accordingly, the synthesis occurs within a vacuum of the order 10^{-5} Torr.

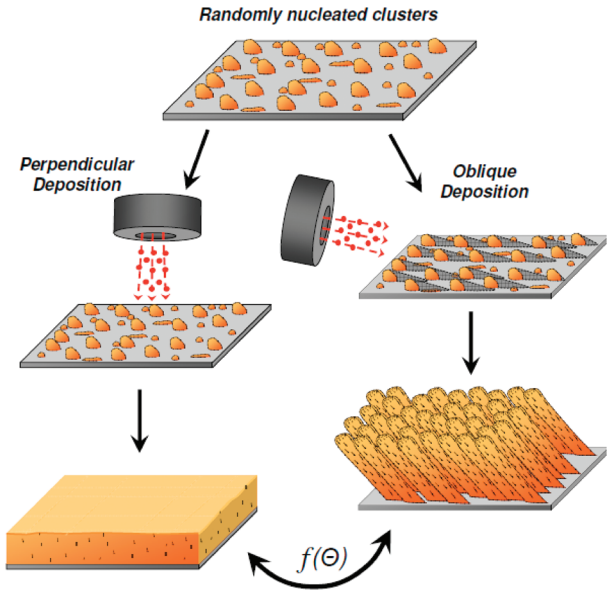

FIGURE 1. Schematic view of RBD demonstrating the manner in which the ultimate film morphology is primarily dependent on the angle of deposition.

The growth proceeds by "hit-and-stick" or ballistic deposition (BD) in which surface diffusion is limited either by cryogenically cooling the substrate or by the presence of strong interactions between substrate and deposited adatoms permitting the formation of kinetically trapped surfaces.[10] During BD, incoming atoms from an evaporation source traverse straight-line trajectories to the substrate and are incorporated in close proximity to their original landing site.[10] Consequently, the method for volatilizing the material must be directional so evaporation achieved by heating the source materials resistively, by electron beam bombardment, or with pulsed laser sources is compatible with BD; however, isotropic deposition methods such as chemical vapor deposition (CVD) or atomic layer deposition (ALD) are not suitable. High vacuum is necessary so that the evaporant mean free path is greater than the distance between the source and deposition substrate. Deposition is stochastic and initial inequities in the local deposition rate result in variations in the film's topography. Deposition along the surface normal forms dense, uniform films because continued deposition over the full geometric area averages out the film thickness with time. However, deposition at oblique angles causes the original topographically elevated points, created randomly, to intercept the flux of subsequent atoms and shadow lower regions, see Figure 1 for illustration.[11,12] This self-shadowing growth process creates porous, columnar films when the rotational orientation about the substrate normal is fixed. Work performed by Brett and co-workers

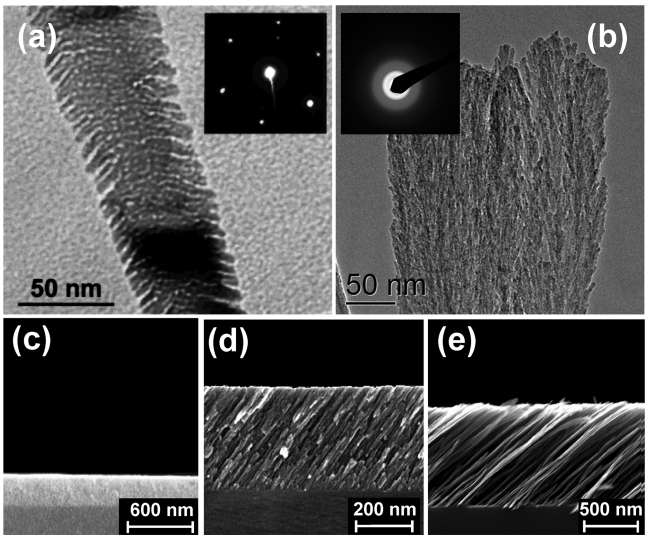

FIGURE 2. Electron microscopy and diffraction of RBD films. (a) TEM of a single MgO column revealing the internal pore structure (inset, electron diffraction pattern illustrating the crystallinity of the column). (b) TEM image of a TiO_2 nanocolumn showing the surface roughness present on the exterior of the column (inset shows electron diffraction pattern demonstrating that TiO_2 is amorphous). (c–e) SEM images of TiC films deposited at angles of 0° (c), 70° (d), and 85° (e) illustrating the progression of film morphology with increasingly oblique deposition angles.

has demonstrated that sculpted helices, springs, and chevrons are generated using glancing angle deposition with rotation about the substrate's azimuthal and polar angles.[12]

RBD follows the geometric principles of BD but extends the control of the material composition by directionally depositing the metallic component in a low-pressure ambient of a nondirectional reactive gas (O_2, C_2H_4, NH_3, etc.). Dohnálek et al. first employed RBD to deposit high surface area MgO films comprised of single-crystal columns, Figure 2a, and since, we have used RBD to grow highly structured films from TiO_2 (Figure 2b),[13–15] TiC (Figure 2c–e),[16,17] α-Fe_2O_3,[18] Sn- and Ti-doped α-Fe_2O_3,[19] and $BiVO_4$,[20] as well as *S*- and C-doped TiO_2, TaN, Mo- and W-doped $BiVO_4$, and Al-doped Co_3O_4.[21] In practice, for a material to be deposited by RBD, all components must be volatilized, one species must be ballistically deposited on the substrate, and the two species must be capable of reaction with one another at the synthesis temperature. Refractory metals can be evaporated by electron beam bombardment of high-purity rods while low-melting point or insulating materials are evaporated by placement within a conductive crucible (molybdenum, tantalum, graphite, etc.), which is then heated by the electron beam, while apertures are used to collimate the evaporant flux. The background gas pressure is selected to provide a flux to the surface, which results in the desired film stoichiometry after considering the dissociative adsorption probability.[13]

Considering the simplicity of the technique, RBD provides significant control over the film structure. Smooth, dense films are produced by directing the flux of the metal species at normal incidence to the substrate. These films possess uniform structure and thickness, because the multitude of independent trajectories necessary to accumulate micrometer-scale films essentially average out small variations. As the deposition angle increases toward more oblique or glancing angles, small variations in local deposition rates become important to the evolution of the film structure. This arises due to the previously mentioned "self-shadowing" effect proposed by Smith et al.[22] Thus, as the trajectory of the directional flux becomes more oblique, the material changes from dense, uniform films, Figure 2c, to continuous, reticulated structures, Figure 2d, and finally into regular arrays of discrete nanocolumns, Figure 2e. This process has been described qualitatively,[11] and ballistic simulations can predict the film structure caused by manipulating the deposition angle and characteristic diffusion length.[23]

Evaporation of a single component in a low-pressure ambient reactive gas generally conforms to the above scheme; however, there are exceptions when multiple components are evaporated simultaneously. One is coevaporation of Bi and V in oxygen at room temperature to synthesize $BiVO_4$, which deviated from the "hit-and-stick" growth mechanism.[20] Coevaporation of Bi and V at normal incidence resulted in reticulated agglomerates of nanowire structures with diameters on the order of 100–300 nm, while deposition at oblique angles (65°) resulted in more directional, jagged features, but not arrays of discrete columns as seen for other materials. This behavior indicates significant adatom diffusion of at least one component (Bi or V) during growth of the films.[20] Of the two components Bi has a much lower melting point temperature and did not react with the oxygen ambient during deposition suggesting that it remained in a mobile metallic state. The absence of discrete nanocolumns with increasing deposition angle demonstrated that the characteristic diffusion distance of Bi adatoms was comparable to the length scale of the film features, ~100 nm, which negates the self-shadowing growth mechanism.[20] Presumably, Bi surface diffusion could be reduced by film growth at sufficiently low temperatures (less than 77 K) to return to a BD-type growth, as seen for Pd films.[24]

RBD may be used to deposit films of varying stoichiometry incorporating a number of different elements, as for $BiVO_4$. This is achieved utilizing multiple evaporative sources or reactive gases simultaneously to form mixed

metal oxides or doped materials. We have grown binary oxide films of Ti–Fe, Sn–Fe, Bi–V, and Al–Co and trinary oxide films of Mo–Bi–V and W–Bi–V by simultaneous deposition of the metals in oxygen.[18–20] This method allows the deposition of materials with precise composition, determined by the flux of the evaporants, assuming a unity sticking probability of the metals, and may be used to vary the composition spatially throughout the film by independently modulating the deposition rates of each component. Moreover, RBD has a distinct advantage over sol–gel or solid-state synthesis methods because multiple metallic components can be combined without being subject to the limits imposed by the equilibrium thermodynamics of mixing since the films are kinetically "trapped" in the BD process. However, this advantage is lost following annealing to sufficiently high temperatures to allow the long-range diffusion of the components, which then are able to segregate. Although other vacuum deposition methods (i.e., CVD and ALD) are capable of producing compositionally well-defined films, these techniques are incapable of producing similarly structured materials due to their isotropic nature. Dopant species such as carbon, nitrogen, and sulfur can be incorporated into films by introducing the appropriate volatile precursors (e.g., ethylene, ammonia, and mercaptans).[21]

The suitability of specific metal–gas combinations for RBD can be tested with a simple experiment. Briefly, the metal flux is directed at a quartz crystal microbalance (QCM) to measure the mass deposition rate of pure metal, and then the reactive gas is introduced at increasingly higher pressures. If a gas and metal are suitably reactive, the mass deposition rate will increase in proportion to the gas pressure until reaching a point of saturation. In some cases, the relative difference in deposition rate in the presence of the reactive gas can be used to estimate the resulting film stoichiometry. During the deposition of metal oxides (i.e., TiO_2, MgO, Fe_2O_3, $BiVO_4$, etc.), oxygen is consumed leaving no byproducts.[9,13,18,19,25] Consequently, the stoichiometry of metal-oxide films estimated by this method was very close to values determined using Auger electron spectroscopy.[13]

Use of RBD To Control Film Properties

Films deposited by RBD have been used by our group as model systems for the investigation of functional materials for the study of photoelectrochemical water splitting and lithium-ion storage. Film thickness, morphology, absolute surface area, pore structure, and crystallinity are important

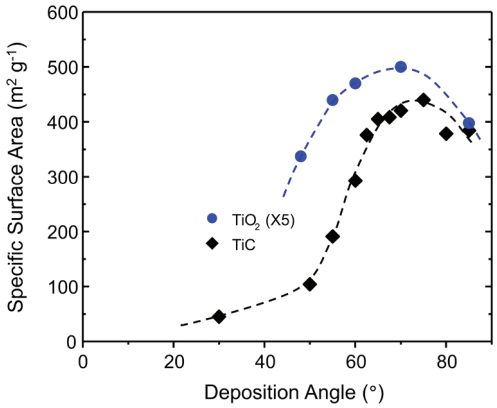

FIGURE 3. Specific surface area of TiO_2 (●), multiplied by five, and TiC (♦) films deposited at 100 and 77 K, respectively.[13,16] Surface area is maximized by deposition at 75° from the surface normal.

characteristics because of their influence on light absorption, electron–hole transfer, ion transport, surface reactions, and mass transfer. An ideal synthetic method would provide the opportunity to independently control structural and compositional parameters to understand structure–property relationships. In order to quantify structural changes such as surface area and porosity of RBD films due to deposition variables, we have primarily utilized two approaches: *in vacuo* adsorption of unreactive gases (N_2 and C_6H_{12}) at low temperatures[9,13,16] and *ex situ* ellipsometry and isothermal adsorption, described below.[15,17,26] Utilizing conditions in which adsorption is strictly limited to a single monolayer and condensation only occurs within pores, the maximum specific surface areas achieved upon optimizing deposition angle and temperature for MgO, TiO_2, and TiC films are estimated to be 1000, 100, and 840 $m^2 \cdot g^{-1}$, respectively.[9,13,17] The specific surface areas, $m^2 \cdot g^{-1}$, of porous TiO_2 films are independent of film thickness indicating that the characteristics of the film structure do not change appreciably with continued deposition. Thus, RBD films can be grown arbitrarily thick to achieve a desired surface area per geometric area without deviating from the growth mechanism.

Due to the self-shadowing effect, the deposition angle dramatically changes the surface area of the films. Figure 3 shows that for films of TiC and TiO_2 the specific surface area increases sharply with increasing deposition angle and achieves a maximum near 75° after which it decreases slightly. The observation of a maximum in the range of 65–75° is a general result attributed to a decrease in the number of micropores able to condense the adsorbate under the experimental conditions,[13,16,24,27] and models of the film growth indicate that the specific surface area will always increase with deposition angle.[23,28,29]

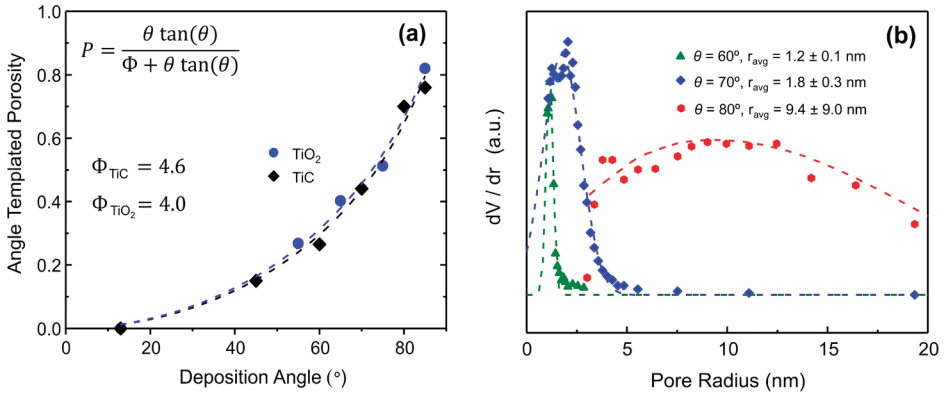

FIGURE 4. Aspects of the porosity of TiO_2 and TiC RBD films deposited at 313 K determined by QCN and EP: (a) porosity of TiO_2 and TiC films as a function of deposition angle, and (b) pore size distributions for TiC films deposited at angles of 60°, 70°, and 80°.[17,21]

Increased rates of surface diffusion result in diminished surface areas for films deposited by RBD because diffusion counteracts the self-shadowing process. In general, an increase in the surface temperature during deposition will negatively affect the surface area due to the increased rate of diffusion. However, in the case of TiC, surface areas increased with deposition until 350 K due to a kinetic barrier for the reaction of ethylene (used as a carbon source) with Ti.[16] Postgrowth annealing, used to improve the crystallinity of the films, induces some loss of surface area; however, bulk diffusion (responsible for structural changes in films after deposition) has a greater kinetic barrier than surface diffusion (the process responsible for surface area loss during deposition). Therefore, as observed with TiO_2, the surface area decreases rapidly as the deposition temperature increases, but postdeposition annealing at equal temperatures induces much smaller changes.[13]

We have also employed quartz crystal nanogravimmetry (QCN) and spectroscopic ellipsometry to measure the surface areas and pore size distributions (PSD) of TiC and TiO_2 films.[15,17] Briefly, RBD films are deposited directly on QCMs, which are mounted in a flow-based adsorption cell coupled with an ellipsometer.[26] Adsorption isotherms of toluene, water, or other adsorbates are acquired by simultaneously monitoring the change in the mass of the adsorbate layer and the optical properties of the film. Data acquired in this way can be treated using BET and Kelvin theory to estimate the porosity, surface area, and PSD of RBD films.[15,17] Additionally, the porosities of RBD films have been determined using ellipsometric porosimetry (EP).[15,17,26,28,30]

The porosity of RBD films, Figure 4a, can be accurately predicted using a simple geometric model, shown in the inset, derived in the limit of low surface diffusion, which utilizes a single fit parameter, Φ, representing the contribution of diffusion during growth.[23,28] The PSD of TiC films is dependent on the deposition angle, Figure 4b, and the mean pore size can be increased by gradually increasing the deposition angle. For deposition angles of 70° or less, the PSD is narrow; however, the width of the distribution rapidly broadens with the mean pore size.[17]

The functional behavior of many materials, especially those for photochemistry as discussed later, relies on the production of specific crystallographic phases or clear evidence of the incorporation of dopants and secondary metals. As a consequence of the hindered mobility of adatoms during synthesis, reactive ballistic deposition of metal oxides at ambient temperatures or lower primarily forms amorphous phases, as seen in the cases of TiO_2,[13] Fe_2O_3,[18] and $BiVO_4$.[25] On the other hand, TiC films deposited at temperatures as low at 77 K grow with significant crystallinity,[16,17] and MgO films grow as highly oriented, single-crystalline columns at 200 K.[9] The released heat of reaction with the background gas will cause localized heating and may account for the crystalline nature of some materials deposited by RBD even at nominally low temperatures.[9,16,17]

RBD Films as Model Electrochemical Energy Conversion and Storage Systems

We have investigated the use of RBD films as electrodes for photoelectrochemical water oxidation[18−20] and lithium-ion storage.[14] The strength of employing the RBD process stems from the ability to independently control several aspects of the film's architecture to create films with different structures but identical composition or to create films with similar structure and different compositions. Additionally, RBD produces adherent films consisting only of the active material allowing for study of intrinsic material properties without

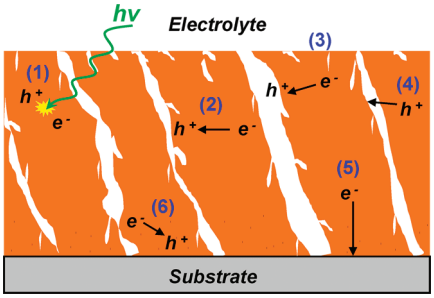

FIGURE 5. Schematic of processes occurring during irradiation of photoactive n-type semiconductor RBD films: (1) absorption of photon generating hole and electron; (2) carrier recombination in bulk, (3) carrier recombination at electrolyte interface; (4) hole transport; (5) electron transport; (6) carrier recombination at substrate interface.

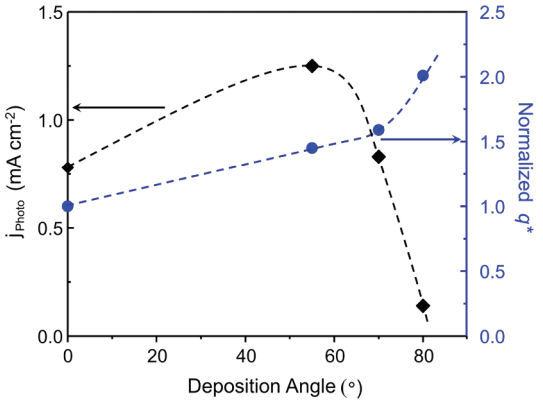

FIGURE 6. Photocurrent at 0.4 V vs RHE and relative film surface area, estimated from voltammetric charge transfer (q^*) during cyclic voltammetry cycles, as a function of deposition angle for α-Fe_2O_3.[18]

complications (and possible misinterpretation) introduced by the presence of binders and conductive fillers required for nanoparticulate systems. These properties enabled us to identify kinetically limiting processes by decoupling the effects of surface area, porosity, and film thickness of the deposited electrodes.[14,18−20]

Photoelectrochemistry. For a system to efficiently convert water into molecular hydrogen and oxygen, it must satisfy several requirements.[31] The materials in the system must possess a sufficiently narrow band gap in order to adsorb a significant portion of the solar spectrum, promote both proton reduction and water oxidation, and remain stable in the electrolyte.[31] To date, no known materials satisfy all of these requirements. The band gap can be evaluated by UV−vis spectroscopy; however, the remaining properties are best determined by the direct evaluation of the material using a photoelectrochemical cell.

The advantage of RBD for these studies is that synthesis parameters such as deposition angle and temperature, film thickness, annealing temperature, and film composition can be manipulated independently. The high surface area resulting from RBD synthesis generates large areas of interface between the film and the electrolyte while simultaneously creating short transport distances for minority carriers generated in the bulk to reach the electrolyte, which generally improves photoefficiency. Additionally, the RBD films can be grown arbitrarily thick to maximize the amount of light absorbed. On the other hand, greater film thickness leads to a higher probability that majority carriers traveling to the substrate may encounter and recombine with minority carriers and reduce the photoefficiency. Figure 5 depicts the charge generation, transport, and recombination processes that determine the efficiency of the material.

Our work on oxides of Fe, Ti, Sn, Co, V, Bi, Mo, and W have demonstrated that RBD can be used to create photoactive, stable, and adherent films of these materials.[18−20] Further, as stated above, the structure of such films is primarily dependent on the growth conditions (deposition angle and temperature) and the postdeposition annealing. In the case of α-Fe_2O_3 films, we demonstrated that photoelectrochemical performance of the films initially improved as the surface area of the film was increased; however, a maximum occurred at a deposition angle of 55° above which the photoefficiency dropped although the surface area of the films continued to increase, Figure 6.[18]

The lack of a monotonic increase of photocurrent with surface area indicates that both electron transport to the substrate (i.e., bulk recombination) and a greater number of defective surface states (i.e., increased surface recombination) were limiting factors in films deposited at the most glancing angles. The former hypothesis was supported by experiments demonstrating that optimum film thicknesses and annealing temperatures existed due to the presence of defects within the film that promoted carrier recombination by hindering electron transport to the substrate. As film thickness increased, absorption of 420 nm light increased monotonically; however the photocurrent saturated in relatively thin films. Additionally, increased annealing temperatures provided greater photocurrents in otherwise identical films indicating improved electron transport. This was particularly important for the thinnest films (<100 nm) in which a greater percentage of the film appeared to be populated with defects due to strain at the substrate−film interface. For thicker films, an optimized annealing temperature was observed at 698−723 K after which the photocurrent decreased substantially due to either a loss of surface area or changes in the nature of the surface sites/defects, both of which

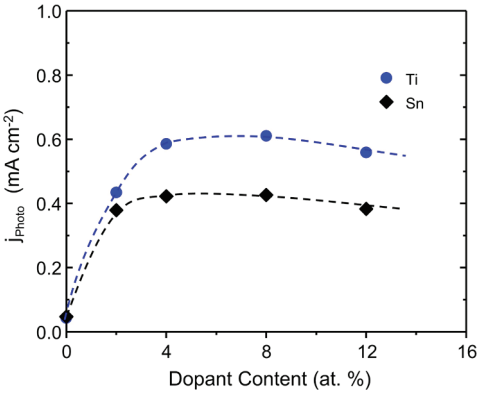

FIGURE 7. Photocurrent at 1.4 vs RHE for RBD α-Fe_2O_3 films deposited at an angle of 75° containing increasing concentration of Ti^{4+} or Sn^{4+} as dopants.[19]

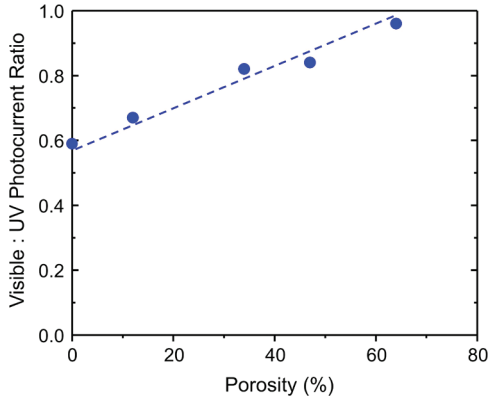

FIGURE 8. Ratio of the contributions of visible to UV light at 1.4 V vs RHE as a function of the film porosity for 4% Ti^{4+} α-Fe_2O_3 films deposited at angles from 0° to 80°.[19]

have been seen to occur on films synthesized by RBD.[9,13,16]

Introduction of metal dopants (Sn^{4+} and Ti^{4+}) was utilized to confirm the hypothesis that electron transport in α-Fe_2O_3 films was a limiting process.[19] Notably, the photocurrent achieved with optimized dopant concentrations, ~8% Sn^{4+} or Ti^{4+}, showed a dramatic improvement of 8-fold and 12-fold for Sn and Ti, respectively (Figure 7), for films deposited at an angle of 75°. The addition of dopant had no distinguishable effect on the optical absorption of the films as shown by UV–vis spectroscopy indicating that the improvement was related to improved electron transport within the film. The addition of Sn^{4+} or Ti^{4+} dopants into α-Fe_2O_3 reduces Fe^{3+} species to Fe^{2+} increasing the n-type conductivity.[32] After incorporation of these dopants, α-Fe_2O_3 RBD films showed little decrease in photocurrent as the film thickness was increased from 180 to 360 nm contrary to undoped α-Fe_2O_3 films, which lost 38% of their activity. Additionally, a stronger field effect at the film–electrolyte interface was identified, which aided in electron–hole separation at the surface, allowing films deposited at more glancing angles, which possess a greater number of surface recombination centers, to exhibit superior photoactivity.[19]

A highly porous or nanocolumnar film allows more visible-light photons to be absorbed relatively close to the electrolyte interface since this interface permeates throughout much of the film, decreasing the required transport distance of the resulting photoholes and reducing their probability of recombining with electrons in the bulk. The ratio of visible to UV photocurrent was observed to increase with increasing deposition angle. In fact, when plotted against the estimated porosity of the films, it shows an almost linear dependence over this range of porosities (Figure 8). This seems to indicate that the nanostructuring brought about by utilizing more glancing angles improves the relative conversion of photons absorbed more deeply within the film, which helps to increase the visible-light conversion efficiency of Ti-doped α-Fe_2O_3.

The ability to identify electron transport as the limiting process would have been difficult using films made by other methods. First, if the films had been produced from sintered nanoparticles then the effects of film thickness would have been correlated with the nanoparticle–nanoparticle interfaces. Second, the addition of dopants was achieved without modifying the synthesis procedure and without changes to the surface area or morphology. Postsynthesis doping methods rely on thermodynamic driving forces for mixing and often result in segregation of the dopant within the film. Here it was shown that the simultaneous deposition of Ti^{4+} or Sn^{4+} with α-Fe_2O_3 leads to a film with homogeneous composition.[19]

Lithium-Ion Storage. Porous materials offer several advantages as Li-ion battery electrodes including increased electrode/electrolyte contact areas, the formation of thinner ion and electron conducting interfacial regions, greater rates of ion-coupled electron transfer due to shorter ion diffusion lengths, and access to both bulk and surface properties.[1,2,4,8] Furthermore, nanosized and disordered materials can accommodate volumetric changes and lattice stresses caused by structural and phase transformations upon lithiation/delithiation.[6] Films deposited by RBD conform to these characteristics, and consequently we have investigated their behavior for Li-ion storage.[14]

Amorphous TiO_2 films were synthesized by RBD directly on copper foils, which obviates the need for binders or

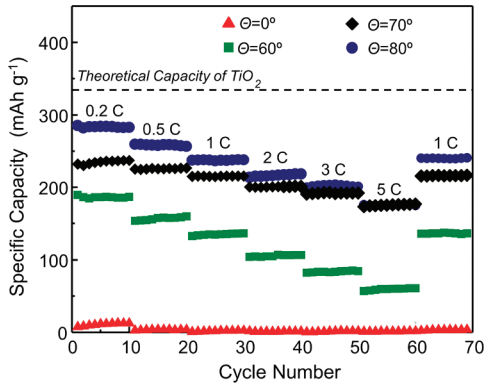

FIGURE 9. Dependence of specific capacity on deposition angle and charge–discharge rate for amorphous TiO_2 films deposited by RBD.[14]

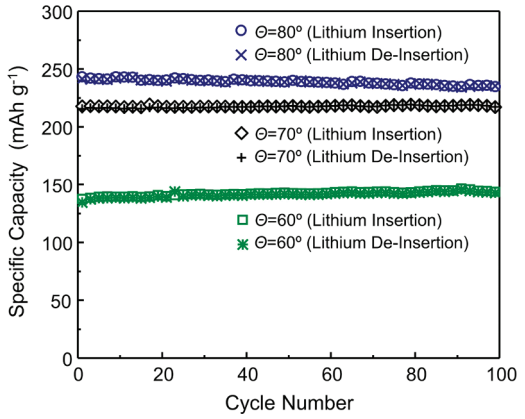

FIGURE 10. Specific capacity of amorphous TiO_2 films as a function of cycle number at charge–discharge rate of 1 C.[14]

conductive additives required in traditional electrode fabrication processes and results in a simpler model system.[14] The films were tested in coin-cell configurations with identical masses of TiO_2; however, the deposition angle was varied between 0° and 80°. Using this approach, we interrogated the effects of morphology, surface area, and porosity on energy density (amount of Li^+ inserted) and rate capability (rate of Li^+ insertion and extraction) for amorphous TiO_2 anodes in lithium ion cells.[14] Films deposited at all angles have the same theoretical capacity for Li^+ insertion as determined by the stoichiometry of the initial electrochemical reduction reaction of TiO_2 by Li^+, and the subsequent insertion–deinsertion cycles are determined by the stability of the lithiated titania phase (i.e., the amount of reversible Li^+ insertion). However, it is clear that the experimentally determined specific capacity (SC) of dense TiO_2 films, deposited at 0°, are an order of magnitude smaller than porous films (Figure 9). Increasing the charging rate, 0.2–5 C (a rate of 1 C indicates full charging or discharging of the cell in 1 h), leads to decreased SC of all TiO_2 films and indicates that diffusion of Li^+ through a Li_xTiO_2 skin is kinetically limiting, and in the case of dense TiO_2, there is little or no bulk lithiation.[14,33] As the porosity of the TiO_2 films are increased, by deposition at increasingly oblique angles, the SC increases monotonically achieving a maximum of 285 mA h g^{-1} at 0.2 C for films deposited at 80°. This result is consistent with the expectation that the most porous and finely divided TiO_2 films, representing the shortest diffusion distances for Li^+ insertion, are created by deposition at the greatest angles, see Figure 4.[17,28]

It is critical that Li^+ insertion anodes be durable and not exhibit degradation in SC with continued charge–discharge cycles. The SC of porous TiO_2 films deposited by RBD is reversible for 100 cycles at 1 C (Figure 10), indicating that the continued insertion and extraction of Li^+ does not lead to significant, irreversible changes in the film structure or integrity. The most porous film, 80°, retained 97% of its initial SC, whereas films deposited at lower angles, 60° and 70°, with lower, yet significant, porosity completely retained their SC.

The charge storage mechanism of porous TiO_2 films contains contributions from both faradaic Li^+ insertion (diffusional) and a pseudocapacitive (surface) response, as well as from nonfaradaic charging of the double-layer, which can be significant for materials with high surface areas.[1] The contributions of each process can be qualitatively distinguished by performing a scan rate dependence using cyclic voltammetry and assuming the rate of Li^+ insertion–diffusion is dependent on $t^{1/2}$ while pure capacitive charging follows t. Films deposited between 60° and 80°, all show a combination of charging due to both Li^+ insertion and the pseudocapacitive effect; however, the charge storage of TiO_2 films deposited at 70° were dominated by pseudocapacitive contributions, which correlates with the earlier observation that the surface area was maximized at this deposition angle.[13,14] Correlations between the charge, Q, and the scan rate reveal that only dense TiO_2 films, deposited at 0°, exhibit diffusion-limited intercalative charge storage behavior. All porous films deposited at oblique angles have high reversible capacity and high rate capability due to both significant surface pseudocapacitive effects and shorter Li-ion diffusion lengths.[14]

Concluding Remarks

The promise of creating functional materials by well-controlled (or directed) synthesis methods that enable precise tuning of dimensionality, mesoporosity, or other types of fine structuring has proven applicability in fields ranging

from Li-ion batteries to heterogeneous catalysis and photoelectrochemistry.[3,4] The reactive ballistic deposition (RBD) growth scheme is one approach for generating adherent thin films with tailored morphology, porosity, surface area, and composition. In short, the angle at which the material is deposited on the substrate controls structural and morphological aspects of the film in the limit of no surface diffusion. The process is applicable to a range of materials with the caveat that they must be made volatile and surface diffusion must be relatively slow. Overall, we have employed the RBD method to change the morphology of a given material from a dense film into continuous, reticulated structures, and finally into uniform arrays of finely structured nanocolumns. This deposition route allows for the systematic control of several material properties including crystallinity, stoichiometry, composition, surface area, and porosity. We have discussed two systems in which the use of RBD grown films were used to deconvolute multiple physical processes to determine the behavior of photochemical processes, the optical properties of materials, and size effects for electrodes for lithium storage. Currently, our group is focusing on using RBD to deposit porous films containing multiple dopants and bulk materials with layered architectures to improve performance for electrochemical energy conversion and storage.

C.B.M. acknowledges the Welch Foundation (Grant F-1436), U.S. Army Research Office (Grant W911NF-09-1-0130), U.S. Department of Energy (Grant DE-FG02-09ER16119) for doped-hematite, and the National Science Foundation (Grant CHE-0934450) for hematite and $BiVO_4$. K.J.S. acknowledges the generous support of the National Science Foundation (Grant CHE-0809770) and the Welch Foundation (Grant F-1529). Z.D. and B.D.K. were supported by the U.S. Department of Energy (DOE), Office of Basic Energy Sciences.

BIOGRAPHICAL INFORMATION

David Flaherty received his Ph.D. in chemical engineering from UT-Austin in 2010 with C. B. Mullins. He is a postdoctoral fellow at the University of California at Berkeley with Professor Enrique Iglesia studying kinetics and reaction mechanisms in heterogeneous catalysis.

Nathan Hahn received a B.S. in chemical engineering from the University of Houston in 2007 and is completing his Ph.D. in chemical engineering at UT-Austin.

R. Alan May received a B.A. in chemistry from Trinity University in 2005 and his Ph.D. in chemistry from UT-Austin under the guidance of Professor Stevenson. He is a postdoctoral fellow at PNNL with Bruce Kay studying chemical physics of supercooled liquids.

Sean Berglund received a B.S. in chemical engineering from Oregon State University in 2003. He worked in microelectronics manufacturing before entering the chemical engineering Ph.D. program at UT-Austin.

Yong-Mao Lin received his M.S. and B.S. degrees in Chemical Engineering at National Taiwan University, Taiwan. He is completing his Ph.D. in chemical engineering at UT-Austin with Buddie Mullins and Adam Heller.

Keith J. Stevenson has been a Professor of Chemistry at UT-Austin since 2000 and conducts research in the electrochemistry of nanomaterials related to energy.

Zdenek Dohnalek is a senior chief scientist at PNNL studying the surface physics and chemistry of catalytic reactions on model single-crystalline and nanostructured surfaces.

Bruce D. Kay has been a Laboratory Fellow at PNNL since 1991. His research interests include heterogeneous catalysis, nanomaterials, and the chemical physics of glasses and supercooled liquids.

Buddie Mullins is Professor of Chemical Engineering and Chemistry at UT-Austin, where he has been since 1991. His research interests include nanomaterials for catalysis, photomaterials, and energy storage.

REFERENCES

1 Arico, A. S.; Bruce, P.; Scrosati, B.; Tarascon, J. M.; Van Schalkwijk, W. Nanostructured materials for advanced energy conversion and storage devices. *Nat. Mater.* **2005**, *4*, 366–377.

2 Maier, J. Nanoionics: Ion transport and electrochemical storage in confined systems. *Nat. Mater.* **2005**, *4*, 805–815.

3 *Basic Research Needs: Catalysis for Energy*; DOE Report, Bethesda, MD, 2007.

4 *Basic Research Needs for Electrical Energy Storage*; DOE Report: Bethesda, MD, 2007.

5 Kamat, P. V.; Tvrdy, K.; Baker, D. R.; Radich, J. G. Beyond photovoltaics: Semiconductor nanoarchitectures for liquid-junction solar cells. *Chem. Rev.* **2010**, *110*, 6664–6688.

6 Sayle, T. X. T.; Ngoepe, P. E.; Sayle, D. C. Simulating mechanical deformation in nanomaterials with application for energy storage in nanoporous architectures. *ACS Nano* **2009**, *3*, 3308–3314.

7 Bruce, P. G.; Scrosati, B.; Tarascon, J. M. Nanomaterials for rechargeable lithium batteries. *Angew. Chem., Int. Ed.* **2008**, *47*, 2930–2946.

8 Luo, J. Y.; Zhang, J. J.; Xia, Y. Y. Highly electrochemical reaction of lithium in the ordered mesoporous β-MnO_2. *Chem. Mater.* **2006**, *18*, 5618–5623.

9 Dohnálek, Z.; Kimmel, G. A.; McCready, D. E.; Young, J. S.; Dohnalkova, A.; Smith, R. S.; Kay, B. D. Structural and chemical characterization of aligned crystalline nanoporous MgO films grown via reactive ballistic deposition. *J. Phys. Chem. B* **2002**, *106*, 3526–3529.

10 Barabási, A.-L.; Stanley, H. E. *Fractal Concepts in Surface Growth*; Cambridge University Press: Cambridge, Great Britain, 1995.

11 Abelmann, L.; Lodder, C. Oblique evaporation and surface diffusion. *Thin Solid Films* **1997**, *305*, 1–21.

12 Hawkeye, M. M.; Brett, M. J. Glancing angle deposition: Fabrication, properties, and applications of micro- and nanostructured thin films. *J. Vac. Sci. Technol., A* **2007**, *25*, 1317–1335.

13 Flaherty, D. W.; Dohnalek, Z.; Dohnalkova, A.; Arey, B. W.; McCready, D. E.; Ponnusamy, N.; Mullins, C. B.; Kay, B. D. Reactive ballistic deposition of porous TiO_2 films: Growth and characterization. *J. Phys. Chem. C* **2007**, *111*, 4765–4773.

14 Lin, Y. M.; Abel, P. R.; Flaherty, D. W.; Wu, J.; Stevenson, K. J.; Heller, A.; Mullins, C. B. Morphology dependence of the lithium storage capability and rate performance of amorphous TiO_2 electrodes. *J. Phys. Chem. C* **2011**, *115*, 2585–2591.

15 May, R. A.; Flaherty, D. W.; Mullins, C. B.; Stevenson, K. J. Hybrid generalized ellipsometry and quartz crystal microbalance nanogravimetry for the determination of adsorption isotherms on biaxial metal oxide films. *J. Phys. Chem. Lett.* **2010**, *1*, 1264–1268.

16 Flaherty, D. W.; Hahn, N. T.; Ferrer, D.; Engstrom, T. R.; Tanaka, P. L.; Mullins, C. B. Growth and characterization of high surface area titanium carbide. *J. Phys. Chem. C* **2009**, *113*, 12742–12752.

17 Flaherty, D. W.; May, R. A.; Berglund, S. P.; Stevenson, K. J.; Mullins, C. B. Low temperature synthesis and characterization of nanocrystalline titanium carbide with tunable porous architectures. *Chem. Mater.* **2010**, *22*, 319–329.

18 Hahn, N. T.; Ye, H.; Flaherty, D. W.; Bard, A. J.; Mullins, C. B. Reactive ballistic deposition of α-Fe_2O_3 thin films for photoelectrochemical water oxidation. *ACS Nano* **2010**, *4*, 1977–1986.

19 Hahn, N. T.; Mullins, C. B. Photoelectrochemical performance of nanostructured Ti- and Sn-doped α-Fe_2O_3 photoanodes. *Chem. Mater.* **2010**, *22*, 6474–6482.

20 Berglund, S. P.; Flaherty, D. W.; Hahn, N. T.; Bard, A. J.; Mullins, C. B. Photoelectrochemical oxidation of water using nanostructured $BiVO_4$ films. *J. Phys. Chem. C* **2011**, *115*, 3794–3802.

21 Hahn, N. T.; Dang, H.; Berglund, S. P.; Hoang, S.; Mullins, C. B. unpublished work.

22 Smith, D. O.; Cohen, M. S.; Weiss, G. P. Oblique-incidence anisotropy in evaporated permalloy films. *J. Appl. Phys.* **1960**, *31*, 1755–1762.

23 Kimmel, G. A.; Dohnálek, Z.; Stevenson, K. P.; Smith, R. S.; Kay, B. D. Control of amorphous solid water morphology using molecular beams. II. Ballistic deposition simulations. *J. Chem. Phys.* **2001**, *114*, 5295–5303.

24 Kim, J.; Dohnálek, Z.; Kay, B. D. Structural characterization of nanoporous Pd films grown via ballistic deposition. *Surf. Sci.* **2005**, *586*, 137–145.

25 Krause, K. M.; Taschuk, M. T.; Harris, K. D.; Rider, D. A.; Wakefield, N. G.; Sit, J. C.; Buriak, J. M.; Thommes, M.; Brett, M. J. Surface area characterization of obliquely deposited metal oxide nanostructured thin films. *Langmuir* **2009**, *26*, 4368–4376.

26 May, R. A.; Patel, M. N.; Johnston, K. P.; Stevenson, K. J. Flow-based multiadsorbate ellipsometric porosimetry for the characterization of mesoporous Pt−TiO and Au−TiO nanocomposites. *Langmuir* **2009**, *25*, 4498–4509.

27 Kimmel, G. A.; Stevenson, K. P.; Dohnálek, Z.; Smith, R. S.; Kay, B. D. Control of amorphous solid water morphology using molecular beams. I. Experimental results. *J. Chem. Phys.* **2001**, *114*, 5284–5294.

28 Poxson, D. J.; Mont, F. W.; Schubert, M. F.; Kim, J. K.; Schubert, E. F. Quantification of porosity and deposition rate of nanoporous films grown by oblique-angle deposition. *Appl. Phys. Lett.* **2008No. 101914.**

29 Smith, R. S.; Petrik, N. G.; Kimmel, G. A.; Kay, B. D. Thermal and nonthermal physicochemical processes in nanoscale films of amorphous solid water. *Acc. Chem. Res.* **201110.1021/ar200070w.**

30 Tompkins, H. G.; McGahan, W. A. *Spectroscopic Ellipsometry and Reflectometry*; Wiley-Interscience: New York, 1999.

31 Bard, A. J.; Fox, M. A. Artificial photosynthesis: Solar splitting of water to hydrogen and oxygen. *Acc. Chem. Res.* **1995**, *28*, 141–145.

32 Anderman, M.; Kennedy, J. H. *Semiconductor Electrodes*; Elsevier: Amsterdam, 1988.

33 Cantao, M. P.; Cisneros, J. I.; Torresi, R. M. Kinetic-study of lithium electroinsertion in titanium-oxide thin-films. *J. Phys. Chem.* **1994**, *98*, 4865–4869.